Tribology Transactions
Publication details, including instructions for authors and subscription information:
http://www.informaworld.com/smpp/title~content=t713669620

Surface Chemistry of Chlorinated Hydrocarbon Lubricant Additives--Part II: Modeling the Tribological Interface

T. J. Blunt [a]; P. V. Kotvis [a]; W. T. Tysoe [b]
[a] Benz Oil, Inc., Milwaukee, Wisconsin
[b] Department of Chemistry and Laboratory for Surface Studies, University of Wisconsin, Milwaukee, Wisconsin

First Published on: 01 January 1998
To cite this Article: Blunt, T. J., Kotvis, P. V. and Tysoe, W. T. (1998) 'Surface Chemistry of Chlorinated Hydrocarbon Lubricant Additives--Part II: Modeling the Tribological Interface', Tribology Transactions, 41:1, 129 - 139
To link to this article: DOI: 10.1080/10402009808983731
URL: http://dx.doi.org/10.1080/10402009808983731

VOLUME 41(1998), 1, 129–139
TRIBOLOGY TRANSACTIONS

Surface Chemistry of Chlorinated Hydrocarbon Lubricant Additives—Part II: Modeling the Tribological Interface©

T. J. BLUNT and P. V. KOTVIS (Member, STLE)
Benz Oil, Inc.
Milwaukee, Wisconsin 53209
and
W. T. TYSOE
University of Wisconsin
Department of Chemistry and Laboratory for Surface Studies
Milwaukee, Wisconsin 53211

In Part I (1), the concept of "Type I" antiseizure behavior for chlorinated hydrocarbons in extreme-pressure (EP) lubrication of ferrous metals was introduced; interfacial temperature measurements and surface analyses revealed that a solid lubricating layer consisting of ferrous chloride ($FeCl_2$) and carbon prevents seizure and acts as a solid lubricant at less than ~1000 K. In this paper, careful measurement of the film growth and removal rates successfully rationalizes this tribological behavior. Thermodynamic calculations also show that iron carbides are favored at higher decomposition temperatures. Analysis of films formed from the thermal decomposition of carbon tetrachloride (CCl_4) and chloroform ($CHCl_3$) at ~1000 K using Mössbauer spectroscopy demonstrates that iron carbide is indeed formed in this case; tribological measurements also confirm this material as critical antiseizure material at high loads in "Type II" tribological behavior for chlorinated hydrocarbons with ferrous metals.

KEY WORDS

Barrier Films, Carbides, Carbon, Extreme-Pressure Additives, Iron, Mössbauer Spectroscopy, Raman Spectroscopy, Solid Lubrication, Thermal Degradation, Thermal Effects

INTRODUCTION

In Part I, surface analytical techniques demonstrated that a film consisting of ferrous chloride ($FeCl_2$) and carbon prevented seizure between rubbing steel surfaces in the pin and v-block apparatus when using model chlorinated hydrocarbons dissolved in polyalphaolefin (PAO). A critical interfacial temperature for seizure was also demonstrated to be about the melting point of ferrous chloride. In addition, a mathematical relationship was established between the applied load and interfacial temperature.

Here, film growth kinetics are measured using identical sources of chlorinated hydrocarbon on polycrystalline iron foils using a microbalance so that temperature and pressure (concentration) effects can be accurately measured. This allows a mechanism for film growth on iron to be determined. Thermodynamic principles can also be used to confirm likely interfacial materials present once the interfacial temperature is determined. Independent determinations of film growth rates by microbalance experiments and removal rates by the pin and v-block apparatus for methylene chloride are successfully used to derive a relationship between seizure load and additive concentration. This is done by assuming that the reactively deposited lubricating film is completely removed when the applied load reaches the seizure load (*2*). Different interfacial materials are then identified as preventing metal-to-metal seizure at the sliding interface. Iron (II) chloride was identified as that crucial material at lower interfacial temperatures (*1*) while iron carbide is identified for the approximate temperature range, 1000–1500 K.

EXPERIMENTAL

Film Growth Apparatus and Procedure

A #2002 Cahn Electrobalance Model RG was used to measure film growth on iron surfaces by reaction of chlorinated hydrocarbons. Figure 1 schematically shows the aluminum microbalance enclosed in a glass chamber along with its controller, a recorder, power supply and separate temperature controller (precision to ±2 K). The enclosing glass envelope is connected to a vacuum line and can be pumped to a mTorr vacuum using a rotary pump. A diffusion pump can then be used to obtain pressures close to a μTorr before heating to the desired temperature. Film growth on the foil was recorded with respect to time and the variation of mass with time was converted to film thickness assuming that the film consists entirely of ferrous chloride. This will not yield accurate absolute values for the thickness of the films although relative values will be accurate (*3*). Absolute weight changes in the foil were also determined using an analytical balance.

Final manuscript approved May 1, 1997

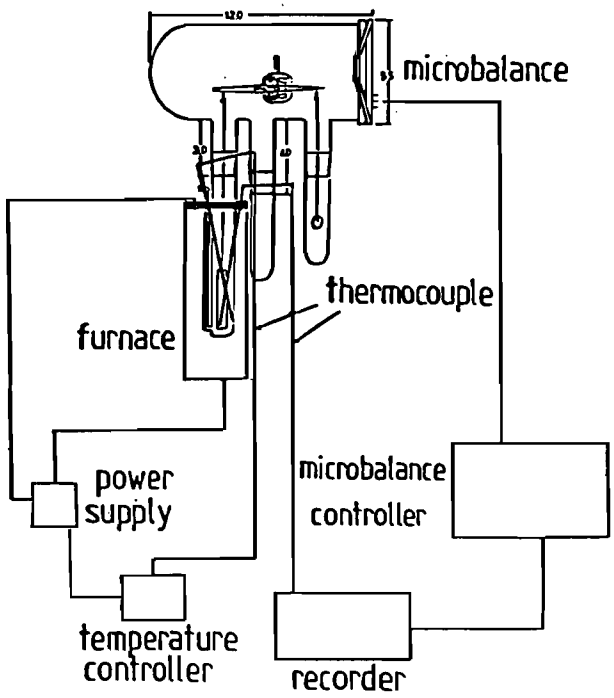

Fig. 1—Schematic diagram of the microbalance used for film growth studies.

Iron foils used for these experiments were obtained from Johnson Matthey Aesar Group with a purity of 99.999 wt.% and 25 μm thickness. They were cut into 10 mm × 30 mm pieces, giving a total surface area ~6×10^{-4} m^2. These were mounted onto the end of one arm of the microbalance using a quartz fiber and grossly balanced using a counterweight attached to the other arm. Standard cleaning procedures for evacuated-microbalance specimens were used on these polycrystalline iron foils.

The chlorinated hydrocarbons were of the highest purity available commercially (typically 99.9+ %; Aldrich Chemical Co.) and stored in glass vials. They were outgassed in vacuum several times prior to use. The same sources of these chemicals were used as for the tribological experiments.

Mössbauer Spectroscopy

Bulk film Mössbauer spectra were recorded on a constant acceleration spectrometer model MS-1200D from Ranger Scientific using a ^{57}Co source in a rhodium foil purchased from Du Pont Merck Pharmaceutical Co. They were collected at room temperature and isomer shifts were quoted relative to iron metal at room temperature. The resulting spectra revealed the presence of cementite, Fe_3C, grown on the iron foils upon exposure to chlorinated hydrocarbon vapors in the film growth experiments above at the same temperatures as those attained tribologically (*4*).

RESULTS AND DISCUSSION

Type I Behavior

Film Growth

Anticipating the balance between film growth and removal as key to predicting seizure, film growth studies under well-defined conditions were conducted in the microbalance to determine the kinetics of film growth as well as the composition of these smooth films. By varying concentration (pressure) and temperature of the chlorinated hydrocarbon in the microbalance, the rate expression for film growth from the chlorinated methane most typical of Type I behavior, methylene chloride (CH_2Cl_2), was derived. Assuming constant film density, Figs. 2 and 3 show the results of typical experiments used to derive the initial film growth rate r_g (in μm/min of ferrous chloride ($FeCl_2$)) for methylene chloride:

$$r_g = A\, p^{1\pm0.1} \exp[(-4.1 \pm 0.2 \times 10^4)/RT] \quad [1]$$

where A is a constant, p pressure (in Torr), R the gas law constant (in Joules) and T the Kelvin temperature. Note from Eq. [1] that the growth activation energy E_a = 41 kJ/mol is in the range expected for chemisorption rather than physisorption. It is much less than the average C-Cl bond strength for methylene chloride (CH_2Cl_2) (*5*). This indicates a catalytic effect for bond scission at the surface of the growing film, based on the assumption that this is the rate limiting step for film growth. The first-order pressure dependence shown in Eq. [1] suggests that this is true.

Comparison of film thicknesses per unit area for three chlorinated methanes is shown in Fig. 4 at a common temperature (746 K). Although chloroform ($CHCl_3$) grew a film on iron significantly more rapidly than methylene chloride (CH_2Cl_2), neither comes close to the rate for carbon tetrachloride (CCl_4). It is important to note that these results show a close correlation to the relative efficacy of these chlo-

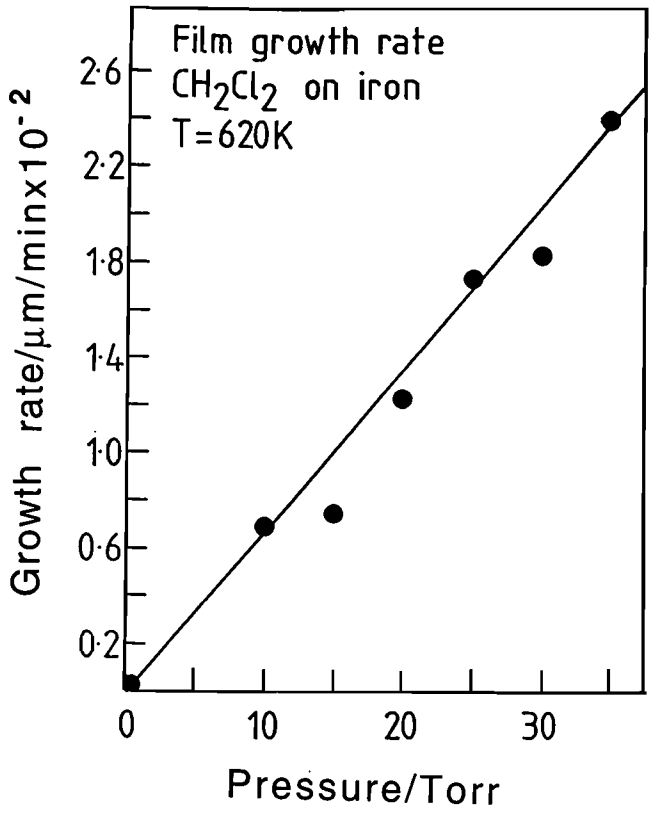

Fig. 2—Plot of film growth rate *vs.* methylene chloride pressure for film growth from the thermal decomposition of methylene chloride (CH_2Cl_2) on an iron foil; its linearity indicates that the reaction order is one for methylene chloride in the rate law expression.

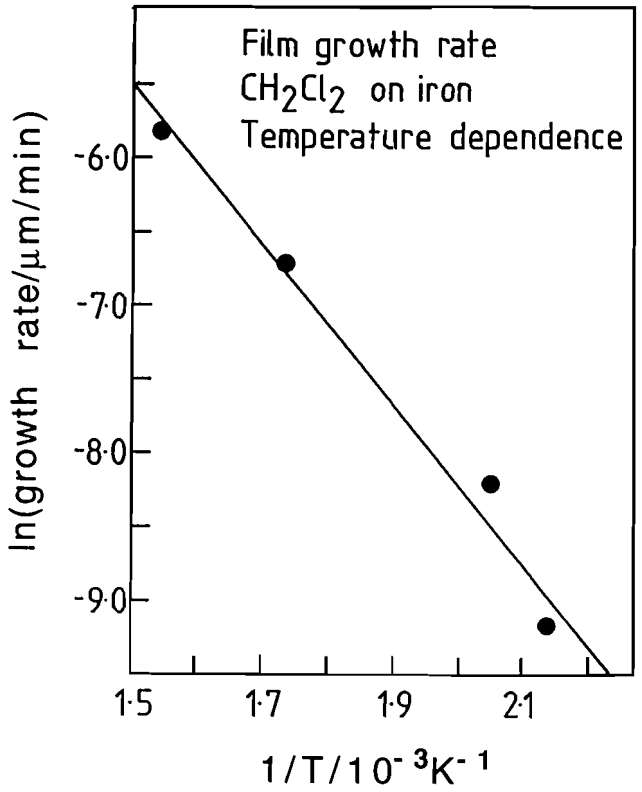

Fig. 3—Arrhenius plot (ln (rate) *vs.* 1/T) for film growth from the thermal decomposition of methylene chloride (CH_2Cl_2) on an iron foil; its slope is equal to the activation energy for film growth divided by *R*. See Fig. 2 for rate units.

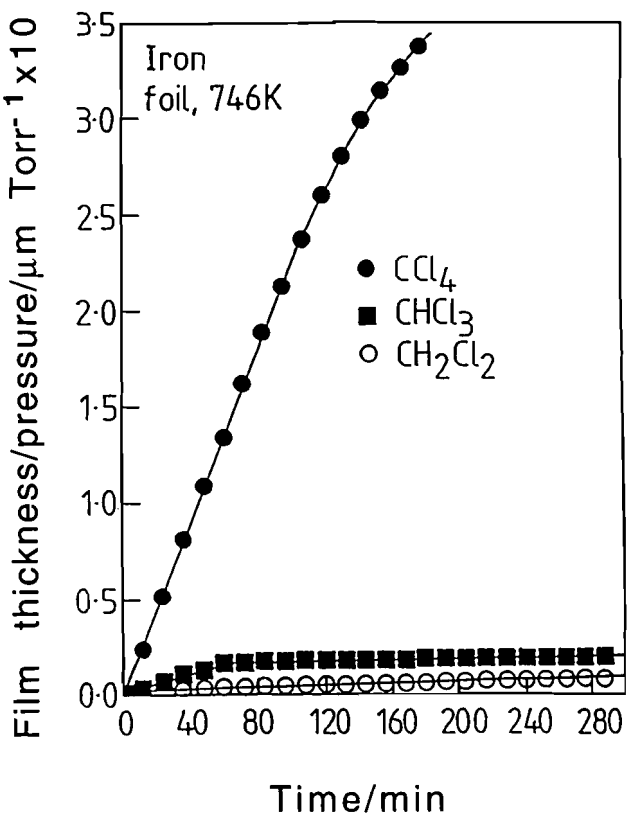

Fig. 4—Plot of average film thickness per unit pressure as a function of time measured in the microbalance for the reaction of carbon tetrachloride (CCl_4), chloroform ($CHCl_3$) and methylene chloride (CH_2Cl_2) vapor with iron foil at 746 K; this thickness in each case has been divided by the pressure of the respective chlorinated hydrocarbon.

rinated hydrocarbons as EP additives (Fig. 2 of Ref. (*1*)). An understanding of differences in the mechanisms of film growth between chloroform and methylene chloride could possibly explain differences in seizure load limits for Type I behavior, i.e., the plateau levels of these response curves, for chlorinated hydrocarbons as a class. Potentially, this understanding could provide the key to understanding effective EP lubrication for other chemistries.

Therefore, determination of film growth kinetics was carried out for chloroform and carbon tetrachloride and the results are discussed in detail elsewhere (*6*), (*7*). Briefly, however, the form of the film growth curve for both chloroform and methylene chloride is given as

$$X = X_m[1 - \exp(-bt)] \qquad [2]$$

where X is film thickness, X_m its maximum for time (t) $\rightarrow \infty$ and b a constant, all of which depend on temperature and pressure (concentration). A rate law expression was derived for chloroform by the same procedures as were used to measure the initial growth rate for methylene chloride as shown in Eq. [1] above. This reveals a similar first-order dependence in the initial growth rate as a function of chloroform pressure. The variation in the maximum film thickness (the value X_m, which is indicated by the presence of plateaus in Fig. 4) was nearly independent of the pressure of chloroform and weakly dependent in the case of CH_2Cl_2 (*6*). This saturation in film growth has been ascribed to the poisoning of active sites for bond breaking on the film surface by carbon. Surprisingly, the growth of films from carbon tetrachloride (CCl_4) did not show the same thickness dependence as Eq. [2], but rather, under suitable conditions, a form was found where

$$X^2 = c\,t, \qquad [3]$$

where c is a constant (*7*). The growth kinetics reverted to a linear law at lower reaction temperatures. Figure 5 shows this parabolic growth form at different temperatures. This is typical for a film growth mechanism where the rate of ion diffusion through the film is the rate determining step (*8*). In addition, since the growth did not saturate at some maximum thickness, site blocking did not appear to be taking place for carbon tetrachloride (CCl_4).

Surface spectroscopies were then performed on these smooth films grown on iron foils. Figure 6 (lower) shows a typical Raman spectrum for methylene chloride and indicates the presence of iron chloride and carbon (see Ref. (*1*) for experimental details of Raman spectroscopy also used there). Similar results are obtained for films grown from chloroform. The broad doublet at ~1350 cm^{-1} and ~1600 cm^{-1} also provides a means to determine the size of these graphitic particles in the iron chloride matrix. The particle size was nearly the same (~50 Å) for both methylene chloride and chloroform (the latter not shown) (*6*). Figure 6 (upper), however, shows the complete absence of carbon particles in films grown from carbon tetrachloride (CCl_4) at these temperatures. Also, the ratio of Raman peak sizes for iron chloride

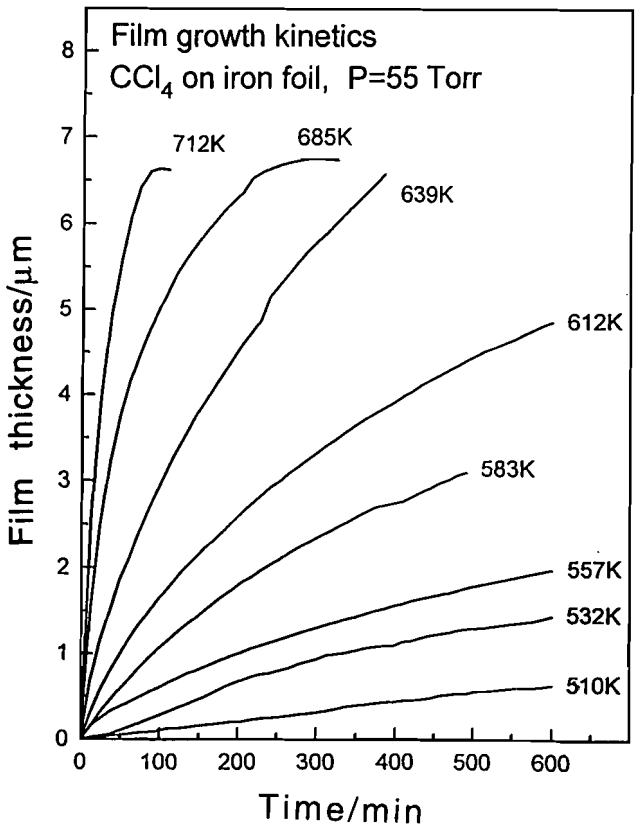

Fig. 5—Plots of film thickness *vs.* time for the thermal decomposition of 55 Torr carbon tetrachloride (CCl_4) on an iron foil measured using the microbalance as a function of sample temperature; these temperatures are marked adjacent to each of the curves.

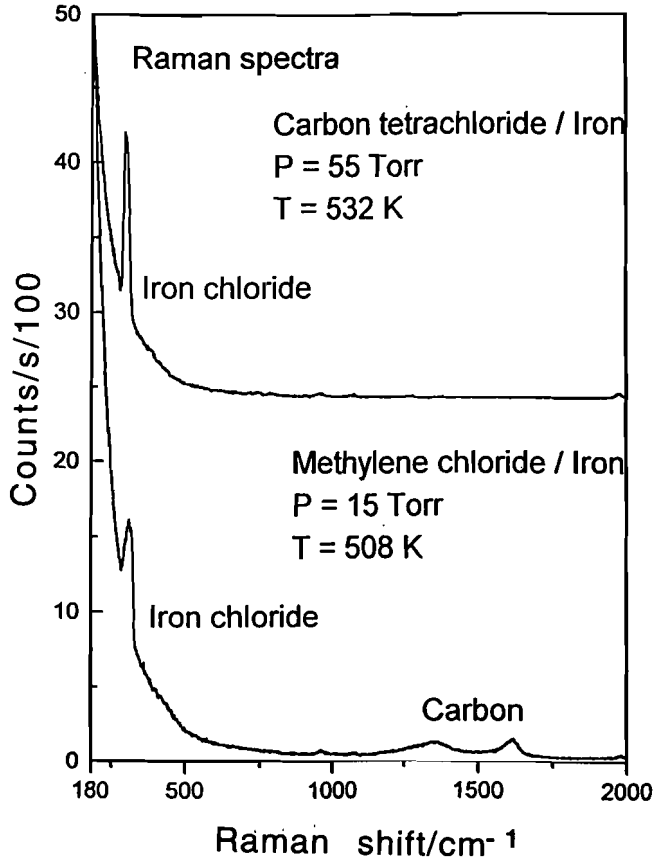

Fig. 6—Raman spectra of films grown on an iron foil by the thermal decomposition of 55 Torr of carbon tetrachloride (CCl_4) at 532 K; shown for comparison is the corresponding spectrum for the thermal decomposition of methylene chloride (CH_2Cl_2; 15 Torr at 508 K).

to the sum of these carbon peaks for chloroform relative to methylene chloride is approximately the same as the Cl:C ratio in the respective additives, i.e., 3:2 (*6*). It is interesting to note that the film growth curves of Fig. 7 for chloroform show an abrupt increase in film growth rate and maximum film thickness as the reaction temperature reaches 600 K. The corresponding growth curves for methylene chloride (CH_2Cl_2) (not shown; (*3*)) and carbon tetrachloride (Fig. 5) show a similar, but less abrupt, change at this temperature. It has been shown by monitoring the carbon coverage on an iron foil in ultrahigh vacuum using Auger spectroscopy that carbon diffuses rapidly into the bulk of the iron sample when it is heated to ~600 K (*4*). This suggests that diffusion of poisoning carbon away from active sites of the growing film and into the iron chloride or metal substrate may cause the increased growth rate above this temperature. This observation is also consistent with the absence of carbon peaks from the upper Raman spectrum of Fig. 6 for the apparently most efficient EP additive, carbon tetrachloride (CCl_4). To further probe this effect, films formed on iron foils by reaction with chloroform and carbon tetrachloride at high temperature were investigated using Mössbauer spectroscopy. This revealed the presence of ferrous chloride ($FeCl_2$), but other peaks were evident in both cases, corresponding to about 15% of the total sample, with an isomer shift δ = 0.19 mm/s and H_{int} = 20.8 T, which are characteristic of cementite Fe_3C (*9*). This observation is consistent with the diffusion of carbon into the bulk of the iron and eventual carbide formation. It is likely that, at the high temperatures attained during extreme-pressure lubrication, the chlorinated hydrocarbon additive completely thermally decomposes to form carbon and iron chloride. This will then lead to a film composition that merely reflects the stoichiometry of the reacting precursor chlorinated hydrocarbon and also rationalizes the relative intensity ratios of the iron chloride and carbon peaks measured in Raman spectroscopy referred to above. This idea has recently been confirmed in molecular beam experiments on clean iron foils in ultrahigh vacuum.

Film Removal

The pin and v-block apparatus was then used to determine removal rates for these films as a function of load. Using a constant speed and time, a form of the Archard wear equation was used (*10*):

$$V = c\,L/S \qquad [4]$$

where V is the wear volume per unit (or constant) sliding distance, c a constant, L the contact load and S the shear strength of the interfacial material, i.e., the grown film separating the steels (*11*) which consists of a ferrous chloride layer which is continually replenished by reaction with the chlorinated hydrocarbon additive. Note, however, that steel is ultimately removed from the surface of the pins and the v-blocks so that V in Eq. [4] refers to the volume of steel

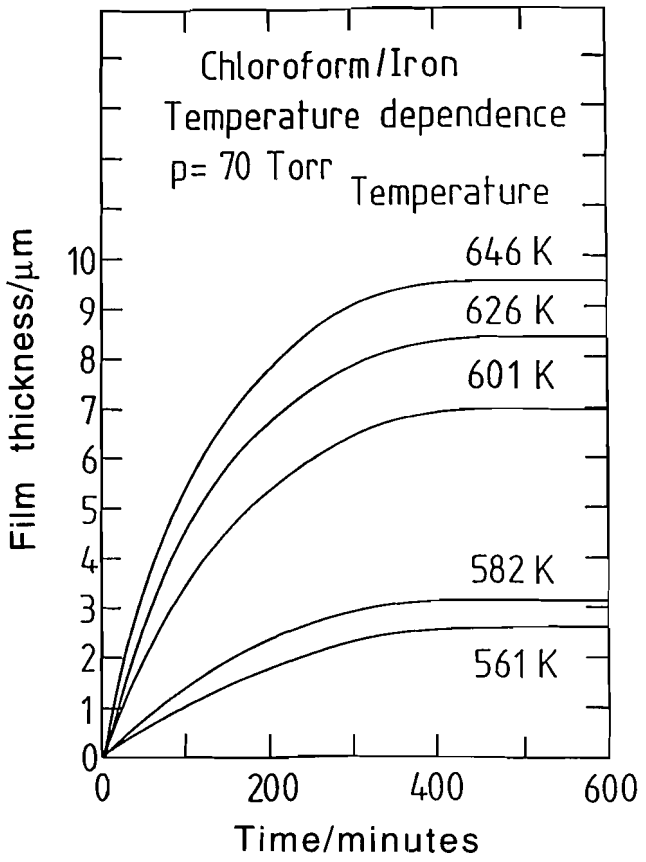

Fig. 7—Film thickness *vs.* time measured using the microbalance due to the thermal decomposition of 70 Torr of chloroform ($CHCl_3$) on iron as a function of sample temperature.

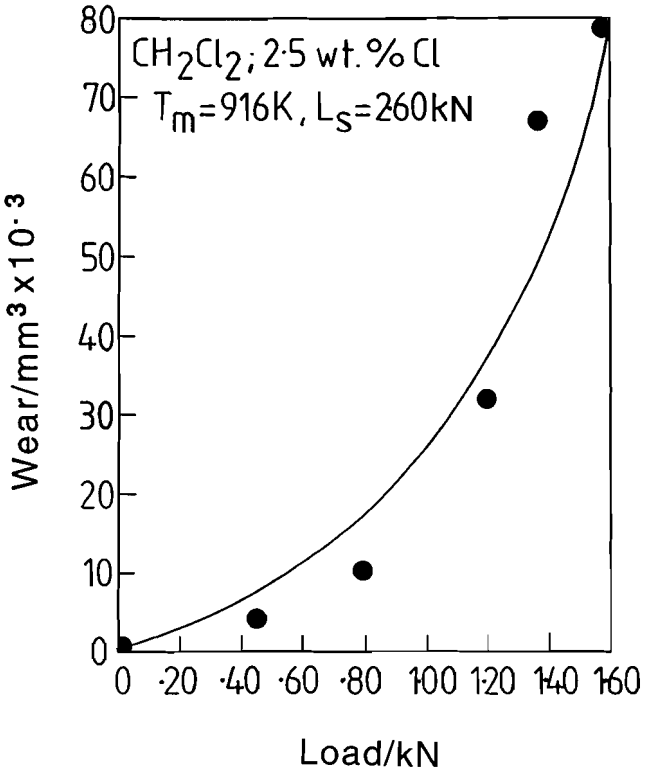

Fig. 8—Plot of volume of material removed in 600 s as a function of load obtained with a pin and v-block apparatus using methylene chloride (CH_2Cl_2) at a concentration of 2.5 wt.% chlorine.

removed. If the rate of film growth represented by Eq. [1] for methylene chloride is greater than the rate of its removal, one would expect effective EP lubrication for suitably smooth surfaces, i.e., no seizure or galling due to metal-to-metal contact. Figure 8 shows the rate of removal of the film grown on the v-block during lubrication by methylene chloride in PAO as a function of load measured in the pin and v-block apparatus. The measurement of wear scars for the constant sliding distance provided the volume of the removed film for the ordinate of Fig. 8 (*3*). The shape of this curve reflects the shear strength dependence on load, and therefore interfacial temperature. Using thermodynamic arguments, Ernst and Merchant derived the temperature dependence of the shear strength as

$$S = S_0 \, ln \, T_m/T \qquad [5]$$

where S_0 is a constant, T_m the melting temperature of the interfacial film and T the interfacial temperature (both in K) (*12*). The interfacial temperature dependence on load for this pin and v-block arrangement was determined in Ref. (*1*) as

$$T = T_0 + a \, L \qquad [6]$$

where T_0 is the bath temperature (322 K), L the direct load in Newtons and the constant a = 0.25 K/N. Combining Eqs. [4] and [5] with Eq. [6] and using a standard least-squares fitting procedure for the data of Fig. 8, the following expression for film removal rate r_r as a function of load can be derived:

$$r_r = \alpha \, L/ln[T_m/(T_0 + a \, L)] \qquad [7]$$

where all constants were separately determined to obtain the best fit and found to be T_0 = 300 K, a = 0.24 K/N, T_m = 916 K and the constant $\alpha = c/S_0 = 1.32 \times 10^{-6}$ mm³/N-min. The corresponding plateau seizure load is indicated in this curve as L_s corresponding to the load at which the interfacial temperature is T_m. These agree well with experimental or previously determined values. Note that the melting point for the interfacial film is somewhat lower than the pure compound (916 K *vs.* 943 K (*13*)) which may be a result of the presence of carbonaceous contaminants in the film. However, the melting point for ferrous chloride ($FeCl_2$) is within a standard deviation of the measured value.

Model for Type I Behavior

By combining the independently derived expressions for film growth and removal rates, the net rate of halide film growth becomes

$$dX/dt = r_g - r_r \qquad [8]$$

This is cast into a numerically soluble equation by using the interfacial temperature dependence on load, Eq. [6], to substitute for T in the film growth expression, Eq. [1], and then by substituting Eqs. [1] and [7] into Eq. [8]). Note that the removal rate in Eq. [7] refers to the wear rate of steel and dX/dt refers to the reactively formed halide film so that these

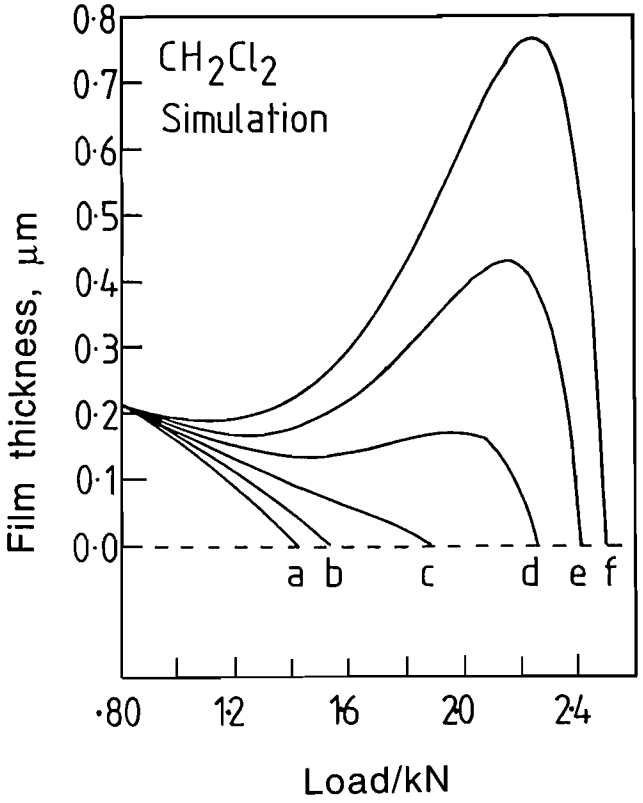

Fig. 9—Theoretical lubricating film thickness at the pin and v-block interface as a function of load using 0.175 wt.% incremental concentrations of methylene chloride (CH_2Cl_2) (a–f), starting at 0.175%.

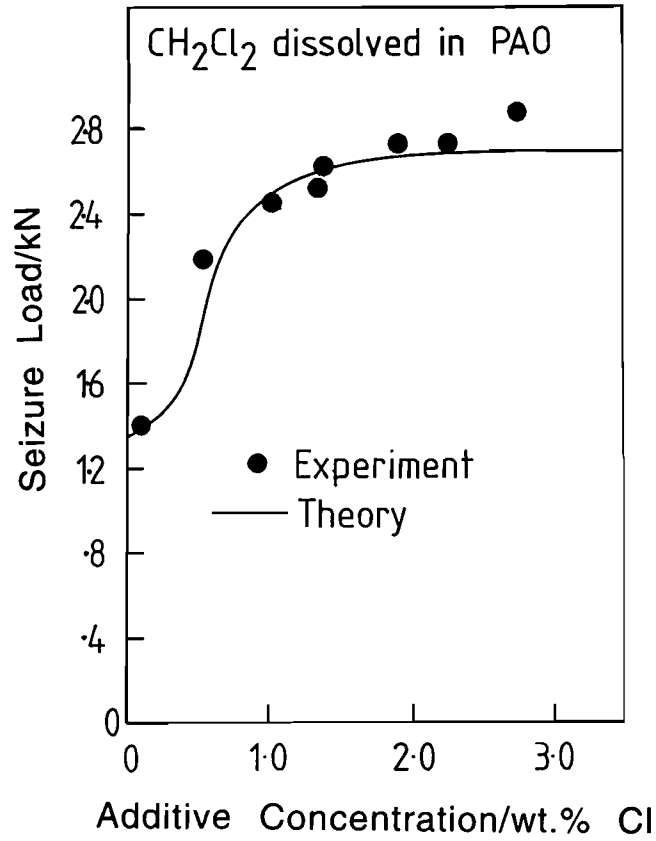

Fig. 10—Theoretical curve for the load at seizure as a function of methylene chloride (CH_2Cl_2) concentration in PAO fitted to the experimental data with the assumption that the lubricating film thickness is zero at seizure.

must be corrected to both refer to halide film thickness. Therefore, solving the general differential equation of Eq. [8] for any additive concentration, and using the linear loading of the contact with time utilized in these experiments, yields the film thickness as a function of load during the experiment (*2*). The result is shown in Fig. 9 for the concentrations (a) to (f) with 0.175 wt.% increments, starting at 0.175%. Partial pressures for the gases of r_g are proportional to concentration here through the ideal gas law and their molecular weights. The zero point constant, i.e., the film thickness at $t = 0$ (assumed to be about the same for all concentrations), was the only adjustable parameter; this value was set at the value of 0.2 μm to obtain the best fit (*3*). This value is nonetheless consistent with the film thicknesses found by the tribological surface analyses of Ref. (*1*). The load where $X = 0$ for any one concentration is then the seizure load. The value theoretically predicted using this model is plotted as a solid line in the seizure load *vs.* additive concentration curve in Fig. 10. Comparison to the methylene chloride (CH_2Cl_2) data in Fig. 2 of Ref. (*1*), i.e., typical Type I tribological behavior, shows good agreement. For convenience, the data of this Part I figure is indicated as solid circles in Fig. 10.

Type II Behavior

General Expression for Interfacial Temperature

Figure 11 shows the analogous chloroform wear rate curve at the same chlorine concentration as that for methylene chloride in Fig. 8. A significantly higher load is asymptotically

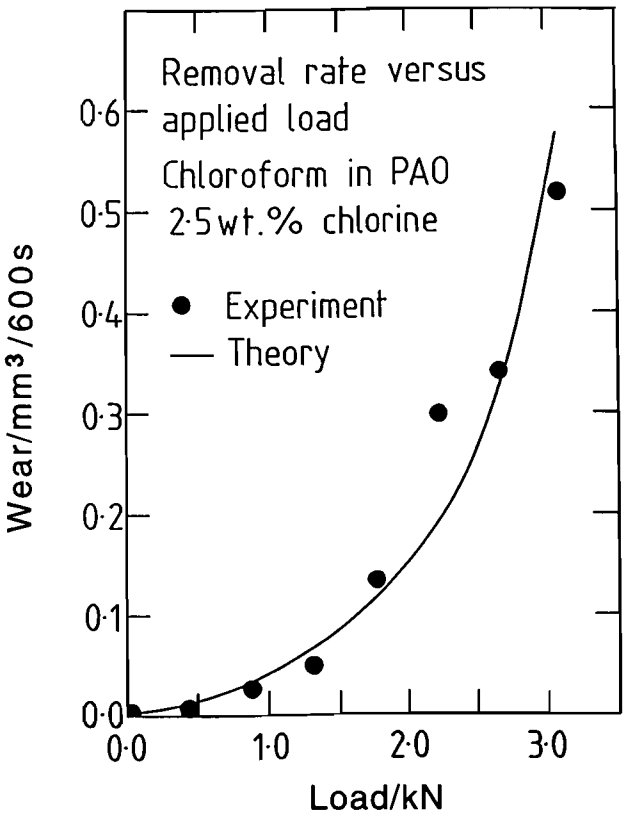

Fig. 11—Plot of volume of material removed in 600 s as a function of load obtained using the pin and v-block apparatus with 2.5 wt.% Cl from chloroform ($CHCl_3$) dissolved in PAO.

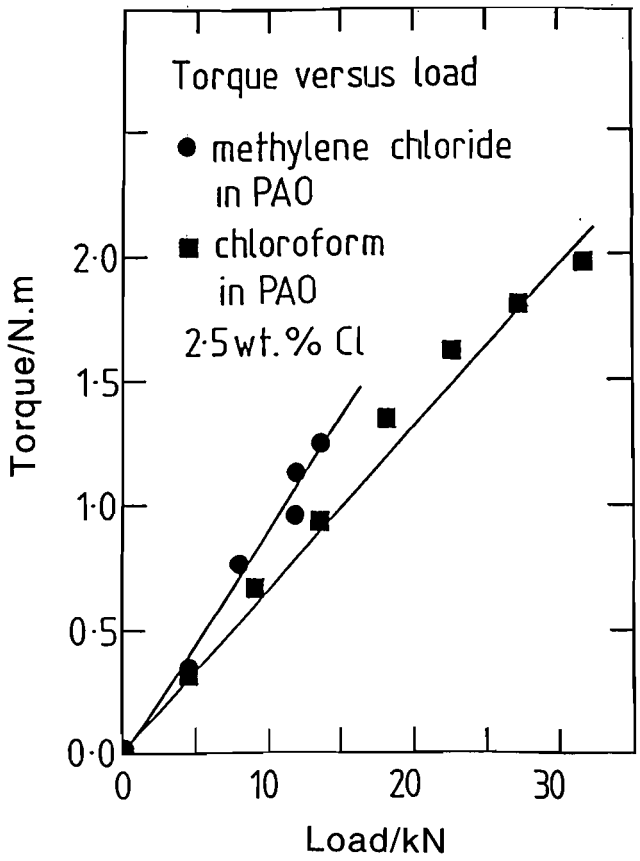

Fig. 12—Plot of torque *vs.* load in the pin and v-block apparatus when using methylene chloride (CH_2Cl_2) and chloroform ($CHCl_3$) as additives. μ = slope × 117 m^{-1} (a geometric factor).

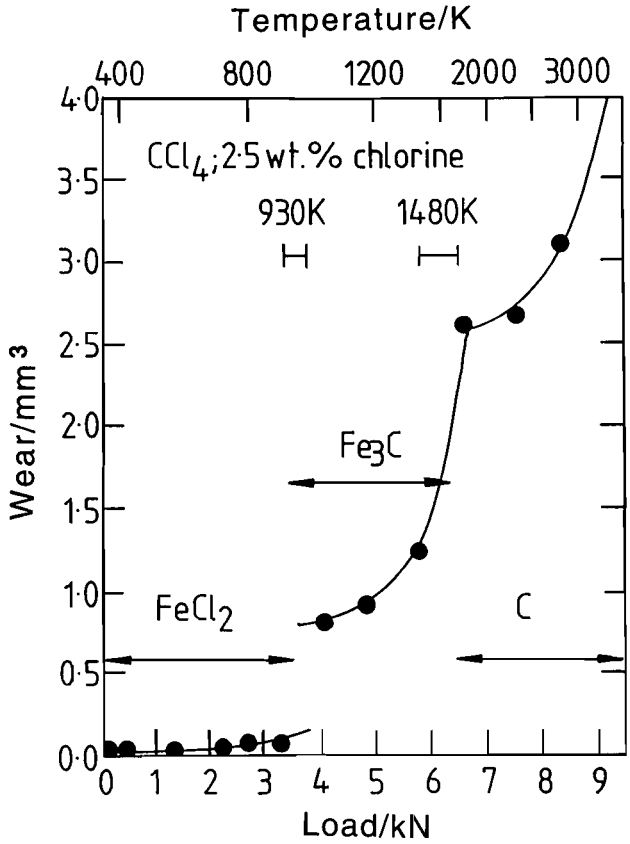

Fig. 13—Plot of the amount of material removed from the surface of the v-block in 600 s *vs.* the applied load in the pin and v-block apparatus for a lubricant consisting of carbon tetrachloride CCl_4 dissolved in PAO using 2.5 wt.% chlorine.

approached in this case. A rigorous derivation of the interfacial temperature as a function of load is given elsewhere (*3*) and shows dependence on the coefficient of friction, as one might expect, since this derivation is simply based on the rate of frictional energy loss in an environment of constant thermal conductivity. A more general relationship corresponding to Eq. [6] that explicitly takes variations in coefficient of friction into account is then:

$$T = T_0 + 0.25[\mu/\mu(CH_2Cl_2)]L \qquad [9]$$

where the expression in brackets represents the ratio of friction coefficients for any lubricant to that for methylene chloride. Equation [9] and friction coefficient determinations, e.g., from the slopes of Fig. 12 for chloroform compared to methylene chloride, explain the higher loads obtainable for chloroform in Fig. 11 (*6*). In addition, such friction coefficient determinations assist in identifying other seizure-preventing interfacial materials as explained below.

Film Removal at High Concentrations and Loads: Carbide Formation

Figure 13 shows the removal rate curve for carbon tetrachloride (CCl_4) at the same chlorine concentration as used for chloroform ($CHCl_3$) and methylene chloride (CH_2Cl_2) above (note that no "plateau" concentration was found for carbon tetrachloride). Included at the top of the plot is the corresponding interfacial temperature calculated from Eq. [9] using the proper friction coefficient for carbon tetrachloride obtained from its torque *vs.* load plot (not shown) (*14*). Also indicated are the apparent critical antiseizure temperatures for different wear regimes and the interfacial materials that correspond to these melting temperatures (*1*), (*15*), (*16*). It is also likely that the PAO diluent itself participates in film formation by contributing carbon, especially at higher interfacial temperatures (*17*). As indicated above, Mössbauer spectroscopy and film growth kinetics are consistent with the movement of carbon into the bulk metal. Ultrahigh vacuum (UHV) surface chemical experiments performed here and by others are consistent with this concept (*18*), as well as the common experience of heat treaters who carbide steels by taking them to the ferrite-to-austenite transition temperature (~1000 K) for hardening them and making them more wear resistant.

Chloroform, when the concentrations are high enough to prevent seizure, also demonstrates Type II behavior like carbon tetrachloride. This is seen in Fig. 14 when concentrations of the chloroform exceed approximately 4 wt.%, below which a "plateau" region characteristic of Type I behavior is seen. Thus, the shape of its plot of wear rate *vs.* load in Fig. 15 differs significantly from its shape at lower concentrations in Fig. 11 and so, for high additive concentrations, is more like that of carbon tetrachloride. The removal curve of Fig. 15 also shows an analogous but much less pronounced transition to higher wear rates near 940 K, ~0.05 mm^3 in 600 seconds, than for carbon tetrachloride in Fig. 13, ~1 mm^3. In these

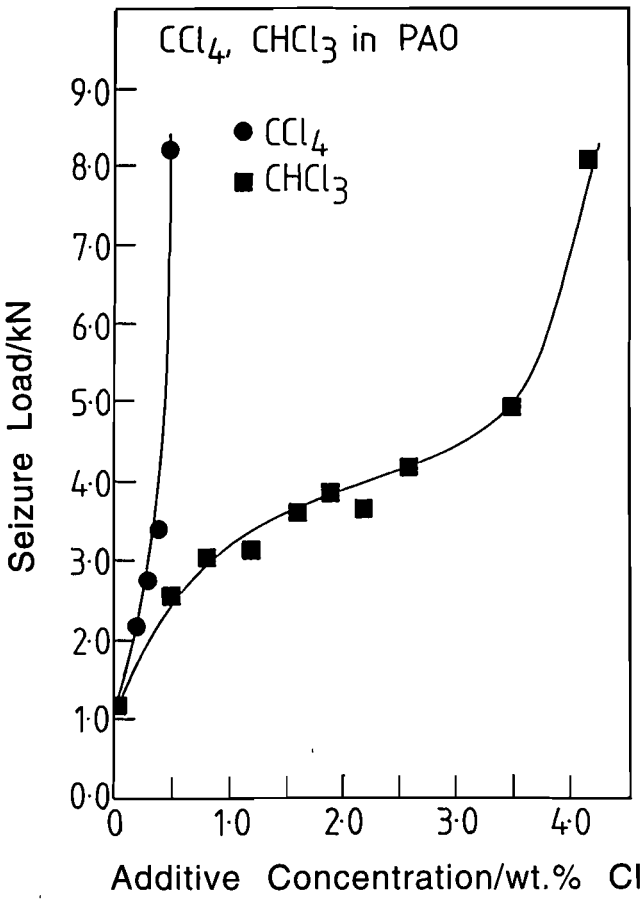

Fig. 14—Plot of seizure load *vs.* additive concentration measured using the pin and v-block apparatus when using carbon tetrachloride (CCl_4; •) and chloroform ($CHCl_3$; ■) as additive dissolved in a polyalphaolefin (PAO).

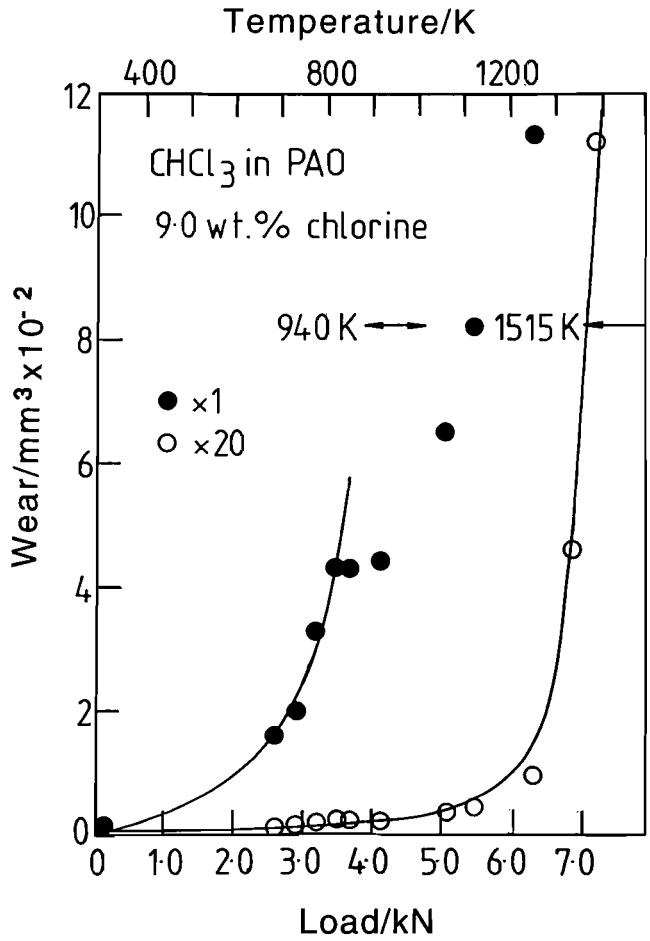

Fig. 15—Plot of the amount of material removed from the surface of the v-block when using chloroform ($CHCl_3$) dissolved in PAO at a concentration of 9.0 wt.% chlorine. Multiplication of open circle wear values by 20 (as indicated) gives the solid circle values consistent with the ordinate shown. Filled circles nonetheless show the break at ~3500 N more clearly while open circles are more consistent with the ordinate scale of Fig. 13.

removal experiments the concentrations of carbon due to the additive alone is 1.0 wt.% [9% × 12/(3 × 35.5)] for chloroform ($CHCl_3$) and 0.2 wt.% [2.5% × 12/(4 × 35.5)] for carbon tetrachloride (CCl_4). The greater concentration of carbon from the additive in the former case, in spite of a lower total carbon content in the resulting test lubricant, may nonetheless cause more carbide formation at the tribological interface than for the carbon tetrachloride experiments, an otherwise better carbide former at the same chlorine concentration, as demonstrated in Figs. 11 and 13. This then may explain the much lower wear rate seen between ~940 and ~1500 K for chloroform in Fig. 15 compared to that for carbon tetrachloride in Fig. 13. This is also in spite of a significantly more "corrosive" environment, i.e., higher chlorine concentration for the chloroform experiments (9%), especially at these high interfacial temperatures. Although this additive carbon could also have a moderating effect on this "corrosive wear" process, in any case the sharp rise in wear rate near ~7400 N for both removal curves corresponds to an interfacial temperature of ~1500 K, very close to the melting/decomposition temperature for cementite, Fe_3C (*19*). Others have more directly measured interfacial temperatures in excess of 1500 K under such extreme pressure tribological conditions in metalworking (*20*).

Thermodynamic verification of this carbide formation phenomenon was sought using a readily available software package (*21*). This program simply minimized the Gibbs free energy for a system containing Fe, Cl and C at any temperature. Figure 16 shows the relative amounts of solid, interfacial materials as a function of temperature calculated by this method. One would expect the relatively soft carbon film to provide little resistance to shear and wear but perhaps protect somewhat against the corrosion represented by $FeCl_2$ formation, also consistent with the region between 1000 and 1500 K in the removal rate curves discussed above (Figs. 13 and 15) and especially for $CHCl_3$. One can also confirm the thermodynamics of carbide formation here simply by coupling this to the iron chloride formation reaction to get a net negative free energy change, a standard technique in physical chemistry (*22*).

Role of Carbon at Lowest and Highest Loads

Carbon appears to play many roles in addition to carbide formation and protection against the rapid ferrous chloride ($FeCl_2$) formation alluded to above at high interfacial temperatures. The Raman spectroscopy results described above reveal the presence of ~50 Å-sized particles when using both chloroform and methylene chloride with a proportionately

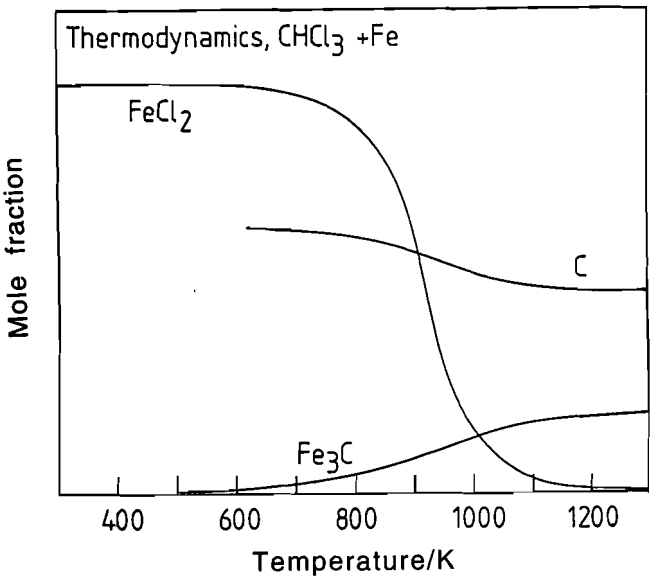

Fig. 16—Plot of the thermodynamically predicted product distribution for the reaction of chloroform ($CHCl_3$) with excess iron as a function of reaction temperature.

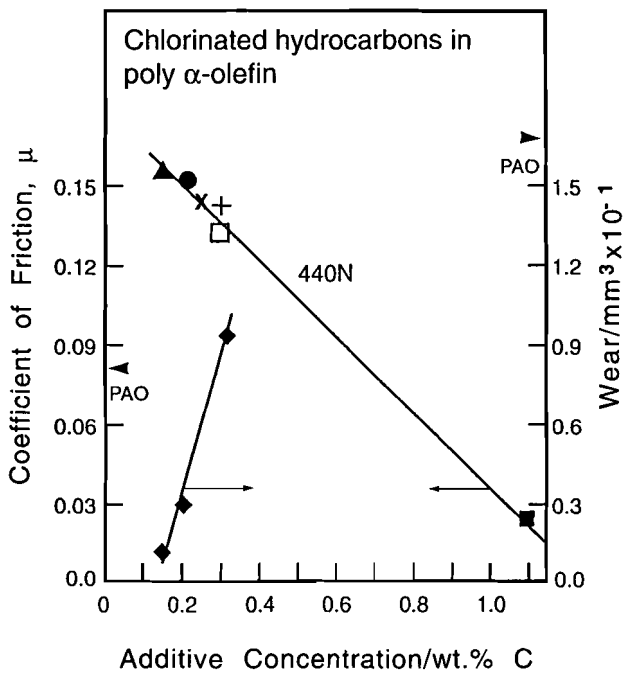

Fig. 17—Coefficient of friction μ and v-block wear volume (♦) after 5400 s as a function of additive carbon content in solution for various chlorinated hydrocarbons dissolved in PAO measured at a load of 440 N. Chlorine concentration is held constant (1.68 wt.%) so that elemental composition is approximately the same for all blends. All other symbols, through which the longest line is drawn, represent different chlorinated hydrocarbons; from left-to-right with decreasing μ, they are carbon tetrachloride (CCl_4; ▲), chloroform ($CHCl_3$; •), hexachloroethane (C_2Cl_6; also •), pentachloroethane (C_2HCl_5; ×) 1,1,1,2-tetrachloethane ($C_2H_2Cl_4$; +), methylene chloride (CH_2Cl_2; □) and 1,4-dichlorobutane ($C_4H_8Cl_2$; ■). The shorter line represents the chlorinated methanes: carbon tetrachloride (CCl_4), chloroform ($CHCl_3$) and methylene chloride (CH_2Cl_2) (left-to-right).

higher particle concentration for the latter, consistent with its relatively higher carbon-to-chlorine stoichiometry. The higher coefficient of friction (μ) for methylene chloride (CH_2Cl_2), as indicated by its greater slope in Fig. 12 compared to chloroform ($CHCl_3$), may then be the result of these carbon particles interfering with the shear planes of the lamellar ferrous chloride (*23*) as these planes slide past one another during lubrication. Higher interfacial temperatures and removal rates at constant load would then also result under these conditions. These friction coefficient differences mean that a lubricant containing methylene chloride as an additive reaches the ferrous chloride melting point more rapidly, i.e., at lower applied loads, during loading to seizure than when chloroform is used as an additive at the same chlorine concentration. This means that the plateau level for seizure load as a function of concentration (Fig. 2 of Ref. (*1*)) is higher when chloroform is used as an additive than when methylene chloride is used (*6*). The lack of carbon in the Raman spectrum of films grown from carbon tetrachloride (Fig. 6) would then also explain its even lower coefficient of friction μ (0.075), as well as wear, and predict that it should display the observed best EP performance. Thus, carbon appears to interfere with effective lubrication at typical EP loads.

Carbide Formation at Asperities

A series of coefficient of friction determinations were also run on several chlorinated hydrocarbons at a much lower load (440 N) but where iron-containing wear debris was nonetheless being generated, see Fig. 17. The measured coefficients of friction are plotted against additive carbon content in solution, i.e., that coming from the additive alone, and show its decreasing, essentially linear, dependence on this content (longer line of Fig. 17). Also shown in this figure are the wear rates for the chlorinated methanes (CH_2Cl_2, $CHCl_3$ and CCl_4) discussed above under these low load conditions (♦). All wear rates for these chlorinated hydrocarbon experiments were, nonetheless, within the range of values indicated by this shorter line, between 0.01 and 0.10 mm^3. The elemental composition for each PAO + additive combination, where the additive concentration is varied to maintain a constant chlorine concentration, was nonetheless approximately the same for these relatively dilute solutions. Of course, the straight PAO carrier, indicated at μ = 0.08 on the left ordinate, contains no chlorine.

Although the shorter line of Fig. 17 indicates that, as predicted above, removal rates for these chlorinated methanes increase with additive carbon content, μ decreases at the same time, contrary to that prediction. The decreasing trend in μ is also seen to extend well past the chlorinated methanes. Also as predicted and mentioned above, however, at much higher loads (1–3 kN), μ correspondingly increases with additive carbon content for the chlorinated methane series (not shown in Fig. 17) (*6*), (*14*). This effect can be explained using the above model of forming halide films, since the surface roughness is largely maintained at these low loads so that now asperities carry most of this load and so experience a severe local EP and temperature condition. This results in their hardening by carbide formation. Therefore, even while wear remains low, indicative of carbide-forming additives μ remains high due to the roughness. This effect is largely missing at higher loads. Note that electron micro-

graphs also confirm a smoothening effect in the sliding direction as load increases under these chemical conditions (*11*). In particular, carbon tetrachloride (CCl_4) prevents wear most effectively while having the highest μ of all those studied. As observed above, it would likely also form carbide most readily under these conditions as well. Thus, carbon appears to decrease wear through carbide formation even under low load, but nonetheless boundary, conditions.

Carbon Accumulation between Asperities

At these low loads the formation and/or accumulation of a soft, low shear strength polymer or other carbonaceous material in the valleys between asperities is also consistent with the above observations concerning Fig. 17. The coefficients of friction for the PAO solutions reflect that it is the carbon from the additive that seems to be directly controlling this property in an essentially linear fashion. Recall the increased surface site poisoning by carbonaceous material with increasing additive carbon content in the film growth experiments above and as demonstrated in Fig. 4. This implies a nonuniform distribution of elements within the growing film depending upon the molecular structure of the chlorine carrier. It also implies that the carbonaceous material from the additive would be found especially in the outermost layers, which are most likely to be displaced into the interasperity region. This is consistent with the decreasing trend in μ with increasing additive carbon content seen in Fig. 17 and is particularly demonstrated by 1,4-dichlorobutane ($C_4H_8Cl_2$; ■). This most complex and highest carbon-containing, chlorinated hydrocarbon shown here provided the lowest, almost hydrodynamic, value for μ. Solid material was nonetheless being removed from the surface but at a much reduced rate from that predicted by an extension of the shorter line of Fig. 17 to the appropriate additive carbon percentage for this additive.

One might expect a low rate of wear for the additives displaying the lowest coefficient of friction, since by Eq. [9] its interface should have the lowest temperature and interfacial material of the relatively highest shear strength by Eq. [5] and therefore lowest wear rate by Eq. [4]. However, this assumes constant interfacial composition. In spite of essentially constant overall lubricant elemental composition, the regularly changing values for μ in these experiments indicate otherwise. Nonetheless, if the additive carbon does not readily form an iron carbide to mediate wear, it appears to moderate wear yielding values much less than predicted by the short chlorinated methane line of Fig. 17 for chlorinated hydrocarbons of longer carbon chain. It would appear to be doing this by filling the interasperity region with a carbon-rich, PAO-insoluble material, displaced from the outermost, carbon-rich layers of the growing asperity film to help bear some of the load.

One can also imagine this surface segregation being destroyed to give a more uniform film as one loads the interface to higher loads, thereby trapping the carbonaceous material while "mixing" it with the more carbon-poor material on the asperities which is being sheared down. This mixing process apparently produces the tribological films of composition reflective of the additive carbon-to-chlorine ratio found previously at higher loads and mentioned above (*6*), (*14*). Evidence of this "filling-in" process is also given by the relatively low value of μ but greatest wear for the PAO alone, as indicated on the ordinates of Fig. 17. In the absence of chlorinated hydrocarbons, the asperity tips, especially as the thin oxide layer is removed to expose bare metal during rubbing, clearly catalyze hydrocarbon decomposition to provide possible filling material for the interasperity region. This decomposition is likely much slower and apparently not a significant factor in the presence of film-covered surfaces derived from chlorinated hydrocarbons, as at least the coefficient of friction data of this figure would indicate.

In spite of the relatively low value for μ, the much higher level of wear for the PAO-only experiment compared to all the others indicates that such material from decomposition is not significantly able to produce an iron carbide layer to mediate wear. In addition, this PAO-derived material cannot prevent catastrophic failure at even relatively low loads (500–1000 N). Thus, in addition to increasing the rate of carbide formation, carbon, coming mostly from the additive, also appears to decrease wear at low loads in a less significant way than carbide formation by providing a low shear, carbonaceous interasperity material to help bear some of the load.

Highest Loads: Unifying Concepts

Under the very high applied loads characteristic of Type II behavior, carbon appears to be playing still another role to prevent seizure, as indicated at the highest loads of Fig. 13. The high wear rates there indicate that both ferrous chloride ($FeCl_2$) and carbide (Fe_3C) are easily removed from the interface above ~1500 K, which suggests the presence of an iron chloride-graphite complex (*24*). This complex or even graphite (C) itself generates a value for μ similar to that found here (about 0.15; (*15*), (*25*)) and happens to be practically the same as the highest values for even the low-load EP data of Fig. 17. Perhaps this similarity indicates the same load-bearing substance is involved in both cases if one cannot, as above, simply invoke the concept of a "roughness component" for μ to explain its highest value in the low-load case.

Stated differently, if the asperity tips bearing the low loads in Fig. 17 have the same film compositions as nearly the entire apparent area of contact for the highest loads of Fig. 13, interasperity contributions to the friction coefficient or frictional force may be negligible, especially in the case of simple chlorinated hydrocarbons (having a small proportion of carbon) dissolved in the PAO, thereby giving $\mu \approx 0.15$ in both high and low load cases. This finding may then simply be a demonstration of the basic tribological principle that contact area is proportional to load. Thus, the coefficient of friction is the same at greatly different loads if the real area of contact has the same composition. Nonetheless, at the highest loads reached in the presence of chlorinated hydrocarbons, where extremely high interfacial temperatures are attained, the hydrocarbon carrier itself may also contribute to carbon deposition (*17*) and even graphitization, since graphite is the preferred carbon form above ~2800 K (*16*). Thus, carbon in the additive appears to be fundamentally affecting μ and wear at all loads. The carbon available from the additive and

its mobility (especially in forming iron carbide) apparently control the direction of its effect at any particular load.

CONCLUSIONS

Ferrous chloride and apparently carbon from chlorinated hydrocarbon additives both play important and varied roles under EP lubricating conditions. It may be rationalized that carbon's availability and movement within the sliding surface reaction layer affects seizure load, μ and wear rates and the transition from Type I to Type II behavior.

ACKNOWLEDGMENTS

The authors gratefully acknowledge the extensive efforts of graduate students, especially Louis Huezo and Javier Lara, for their film growth work as supported by the Analytical and Surface Chemistry Division of the National Science Foundation under Grant No. CHE-9213988 and K. Surerus for collecting Mössbauer spectra. Special thanks also to Ms. Bonnie Roznik for expert manuscript review and suggestions. The excellent electron microscopy of Prof. M. N. James of the University of the Witswatersrand, Johannesburg, South Africa, is also gratefully acknowledged.

REFERENCES

(1) Kotvis, P. V. and Tysoe, W. T., "Surface Chemistry of Chlorinated Hydrocarbon Lubricant Additives—Part I: Extreme-Pressure Tribology," *Trib. Trans.*, **41**, 1, pp 117–123, (1998).

(2) Kotvis, P. V., Huezo, L. A., Millman, W. S. and Tysoe, W. T., "Highly Chlorinated Methanes and Ethanes on Ferrous Surfaces," in *Surface Science Investigations in Tribology*, Chung, Y.-W., Homola, A. M. and Street, G. B., eds., American Chemical Society, Washington, D.C., pp 144–55, (1992).

(3) Kotvis, P. V., Huezo, L. A. and Tysoe, W. T., "Surface Chemistry of Methylene Chloride on Iron: A Model for Chlorinated Hydrocarbon Lubricant Additives," *Langmuir*, **9**, p 467, (1993).

(4) Kotvis, P. V., "Film Growth and Extreme Pressure Tribology of Chlorinated Hydrocarbons on Ferrous Metal Surfaces," Ph.D. Dissertation, University of Wisconsin-Milwaukee, Milwaukee, WI, (1991).

(5) Cox, J. D. and Pilcher, G., *Thermochemistry of Organic and Organometallic Compounds*, Academic Press, New York, pp 398–399, (1970).

(6) Huezo, L. A., Kotvis, P. V., Crumer, C., Soto, C. and Tysoe, W. T., "Surface Chemistry and Extreme Pressure Lubricant Additive Properties of Chloroform on Iron," *Appl. Surf. Sci.*, **78**, p 113, (1994).

(7) Lara, J., Molero, H., Ramirez-Cuesta, A. and Tysoe, W. T., "Structure and Growth Kinetics of Films Formed by the Thermal Decomposition of CCl_4 on Iron Surfaces," *Langmuir*, **12**, p 2488, (1996).

(8) Cabrera, M. and Mott, N. F., "Theory of the Oxidation of Metals," *Rep. Prog. Phys.*, **12**, p 163, (1949).

(9) Tysoe, W. T., Surerus, K., Lara, J., Blunt, T. J. and Kotvis, P. V., "The Surface Chemistry of Chloroform as a Extreme-Pressure Lubricant Additive at High Concentrations," *Tribology Letters*, **1**, p 39, (1995).

(10) Rabinowicz, E., *Friction and Wear of Materials*, John Wiley, New York, p 137, (1965).

(11) Kotvis, P. V., Tysoe, W. T. and James, M. N., "An Investigation of Film Removal in Extreme Pressure Lubrication Using Chlorinated Hydrocarbon Additives," *Wear*, **53**, p 305, (1992).

(12) Ernst, H. and Merchant, M. E., "Surface Friction of Clean Metals—A Basic Factor in the Metal Cutting Process," *Proc. Special Summer Conference on Friction and Surface Finish*, MIT Report No. 15, MIT Press, Cambridge, MA, p 76, (1940).

(13) *CRC Handbook of Chemistry and Physics*, Lide, D. R., ed., CRC Press, Boca Raton, FL, pp 4–6, (1993).

(14) Kotvis, P. V. and Tysoe, W. T., "The Nature of the Lubricating Films Formed by Carbon Tetrachloride Under Conditions of Extreme Pressure," *Wear*, **201**, p 10, (1997).

(15) Chinowsky, S., *ASM Handbook*, **18**, ASM International, Materials Park, OH, pp 816–819, (1992).

(16) Cook, M. W., "A Guide to Machining Carbon and Graphite with Syndite PCD," *Industrial Diamond Review*, **54**, 563, p 174, (1994).

(17) Koch, B., "Thermal Stability of Synthetic Oils in Aviation Applications," *Jour. Syn. Lubr.*, **6**, p 275, (1990).

(18) Smentkowski, V. S., Cheng, C. C. and Yates, J. T. Jr., "The Interaction of Carbon Tetrachloride with Fe(110): A System of Tribological Importance," *Langmuir*, **6**, p 147, (1990).

(19) *CRC Handbook of Chemistry and Physics*, Lide, D. R., ed., CRC Press, Boca Raton, pp 5–65, (1991).

(20) Bhattacharya, S. K., Aspinwall, D. K. and Nicol, A. W., "The Application of Polycrystalline Compacts for Ferrous Machining," in *Proc. 19th Int'l. Machine Tool Design and Res. Conf.*, p 425, (1979).

(21) "HSC Chemistry," Version 2.0, Outokumpu Research, Pori, Finland, pp 35–57, (1994).

(22) Castellan, G. W., *Physical Chemistry*, Addison-Wesley, Reading, MA, p 224, (1964).

(23) Wyckoff, R. W. G., *Crystal Structures*, **1**, Interscience, New York, pp 270–2, (1963).

(24) Cotton, F. A. and Wilkinson, G., *Advanced Inorganic Chemistry*, 3rd ed., Interscience, New York, p 290, (1972).

(25) Rabinowicz, E., *Friction and Wear of Materials*, John Wiley, New York, p 81, 93, (1965).